



IJRASET

International Journal For Research in
Applied Science and Engineering Technology



INTERNATIONAL JOURNAL FOR RESEARCH

IN APPLIED SCIENCE & ENGINEERING TECHNOLOGY

Volume: 5 Issue: XII Month of publication: December 2017

DOI:

www.ijraset.com

Call:  08813907089

E-mail ID: ijraset@gmail.com

Optimal Design of Filament Wound ISO-grid Composite Lattice Cylindrical Structure Using Buckling and Vibrational Analysis

Anthony Johnson Yesudas¹, Amalesh Barai², V KalyanChakravarty³

^{1,2}Institute of Aeronautical Engineering, Hyderabad 500 043

³Advanced Systems Laboratory, Hyderabad 500 058

Abstract: Advance grid stiffening is the most structural efficient and lightweight method employed extensively in the composite structures. The phenomenon of Eigen buckling of iso-grid composite lattice cylindrical structures plays the vital role which undergoes critical bonding between the shell and the iso-grid stiffeners. An iso-grid lattice 3D finite element models have been studied up to optimal design configurations with different parameters of the shell and the iso-grid stiffeners. The investigation is performed using finite element analysis under uni-axial compressive loads and catastrophic effects are detected. Various failure modes are observed such as global buckling, local buckling & stiffener crippling. Vibrational behavior i.e., natural frequencies and harmonic response of the iso-grid lattice structures are investigated. The effect of geometrical parameters and materials properties of iso-grid stiffeners is studied on the various vibration characteristics. Obtained numerical results with respect to the parameters are plotted using graphs.

Keywords: Advance grid stiffening, Iso-grid Lattice Cylinder, Eigen Buckling, Finite Element Analysis & Vibrational behavior.

I. INTRODUCTION

The major concern in today's automotive, aerospace and aircraft industries is structural efficiency and the vibrational behavior of structures is also great significance in structural dynamics. Therefore, this need for structural efficiency can be overcome by the use of robust and lightweight materials. To this extent, an advanced grid-stiffened structure with their high specific strengths discovers wide application. Cylindrical structures made up of composite material are used in the aerospace and aircraft industries especially in the form of the aircraft fuselage and launch vehicle fuel tanks. Hence, the practice of composite materials in various engineering fields like aerospace manufacturing extended significantly in current years. Usage of material in the manufacturing of aerospace structures as a replacement for metallic materials, that tends to the reduction of mass by up to 30%. Remarkable use of filament winding device for producing composite shells in the aerospace field[1].

A. The History of Grid-Stiffened structures

The early precursor of current advanced grid-stiffened structure which is principal aluminum is o-grid is improved by McDonnell-Douglas Corporation as it holds the patent rights. A single piece of aluminum stock is used to machine the structure and it consists of a skin made of stiffeners, which form equilateral triangles. The Prefix "iso" is derived from the stiffness activities of an is o-grid is isotropic within the plane of the structure. These structures are still used as the source for the Titan, Atlas, Delta launch vehicle shrouds and interstates, despite being recognized several decades ago[2]. Preliminary design and analysis are founded on a continuum model where stiffening ribs are smeared, based on rib spacing, to reach an equivalent shell and also used rib spacing in relative to rib cross-sectional width as the standard to smear the ribs [3]. A new technique was offered to investigate the Advance grid structure in which the components of equations stress-strain was advanced by the several grid patterns [4]. On various grid structures, the behavior was predicted by deformation and failures of the lattice structures [5]. An investigation on Eigen buckling of the composite lattice cylindrical structure along with independent grid cell and forces acted on ribs of skin are computed normally cylindrical skin stiffness matrices (A, B & D) and there are verified with experimental and analytical results concluded [6]. Adoption of smearing the stiffener with diverse conditions that are the equivalence of strain energy, stiffness contribution (through force & moment study), rib spacing, etc. Where ass hear and transverse strains remain ignored in few authors, a smeared stiffeners model that interpretations for transverse shear flexibility [7], [8], [9]. The degree of precision anticipated and bound of computational cost, three kinds of buckling analysis are been investigated. Linear bifurcation analysis is the elementary analysis sort that is not considered the stresses and prebuckling deformation [10]. In the second method of bifurcation analysis takes into consideration the

stresses and nonlinear prebuckling outcomes in far more exact buckling load. Where as in the third kind of analysis, the nonlinear buckling analysis, permits for large nonlinear geometric deflections. An investigation on vibrations of stiffened cylindrical shells with grid structure under full free boundary conditions are analyzed on the approximation of love theory and After simplification of equilibrium equations, the shell frequency equation is obtained by using Galerkin method [11].The research was done on the free vibration problem for the isotropic cylindrical shells with varying ring-stiffener distribution using the extended Ritz method [12].Exploration of different boundary conditions; have analyzed the influence of stiffeners on natural frequencies of stiffened cylindrical shells. Here the investigations of stiffeners are considered as discrete elements, energy method and Hamilt on principle are used to obtain equations of motion [13].

II. ANALYTICAL MODEL

To define the equal extensional, coupling and bending of the complete stiffened structures in demand to calculate the global buckling load of the grid stiffened. It includes defining the stiffness impact of the stiffener. The smeared technique is a procedure of decreasing the stiffened cylinder into an equal laminate. A thorough framework of the phases trailed to progress the analytical model and the expectations through stand accessible underneath. In evolving the analytical model, a unit cell of the stiffener structure takes to be defined ahead. The unit cell is designated such that the entire iso-grid cell can be duplicated by replication of this unit cell [6].

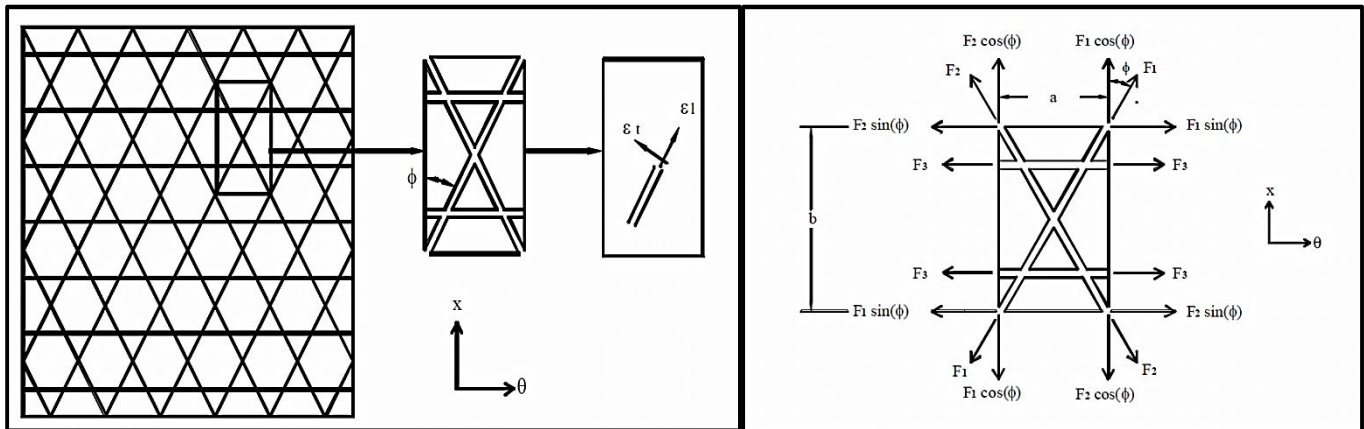


Fig.1 Unit cell and coordinate system

Fig.2 Force diagram

Primarily a unit cell is well-defined and the corresponding parameters are given for that unit cell and that specific unit cell is duplicated into a cylinder panel. It is the way to produce the effective complete panel through a unit cell as shown in Fig.1. In essential the stiffness effect of the stiffeners toward the entire structure, at this point the analysis is to be complete according to force and moment collaboration of the stiffeners. The thorough stiffness of the panel remains at that point supposed by smears toward the stiffener and the shell stiffness parameters permitting to the volume fraction of each individual. Now direction to perform the superposition of the A, B and D matrix (equivalent extensional, coupling and bending matrices) of the shell and stiffeners, the constitutive equation enlightened for the stiffeners necessities towards the position of the shell a purpose of the midplane strains and curvatures. In evolving this analytical model, the consequent outlooks are arranged.

- 1) Unidirectional stiffeners consisting transverse modulus is significantly lesser than the longitudinal modulus, and the cross-sectional dimensions stand likewise similar minor related to the length measurement; consequently, the stiffeners remain anticipated toward provision axial load merely.
- 2) The strain is constant crosswise the cross-sectional area of the stiffeners. Therefore constant stress dispersal is recognized.
- 3) The load is conveyed over shear forces among the shell and the stiffeners.

A. Force Distribution[6]

Heremid planecurvatures and strains of the skin stand specified by $k_x^0, k_\theta^0, k_{x\theta}^0$ and $\epsilon_x^0, \epsilon_\theta^0, \epsilon_{x\theta}^0$ correspondingly. The equivalent strains on the innermost surface of the shell are detailed in expressions of the mid plane strains and curvatures through equation (1) [14]. Meanwhile the stiffeners remain complex toward the skin on this boundary; the strains by this boundary stand used as the matching state on behalf of the stiffener and the shell.

$$\begin{aligned} \varepsilon_x &= \varepsilon_x^0 + k_x (t/2) \\ \varepsilon_\theta &= \varepsilon_\theta^0 + k_\theta (t/2) \\ \varepsilon_{x\theta} &= \varepsilon_{x\theta}^0 + k_{x\theta} (t/2) \end{aligned} \tag{1}$$

Here ‘t’ is the thickness of the shell. The strains achieved by Equation (1) essential to be resolute along the stiffeners directions meanwhile these remain the related strains. It is ended by premultiplying the border strains through the conversion matrix Equation (2) [15]. These outcomes in strains throughout the stiffener direction ε_l , normal to the stiffener directions ε_t and agreeing shear strain ε_{lt} Fig.1.

$$\begin{bmatrix} \varepsilon_l \\ \varepsilon_t \\ \varepsilon_{lt} \end{bmatrix} = \begin{bmatrix} c^2 & s^2 & sc \\ s^2 & c^2 & -sc \\ -2sc & 2sc & c^2 - s^2 \end{bmatrix} \begin{bmatrix} \varepsilon_x \\ \varepsilon_\theta \\ \varepsilon_{x\theta} \end{bmatrix} \tag{2}$$

Where $c = \cos(\alpha)$, $s = \sin(\alpha)$ and α stands the stiffener orientation angle.

Accordance with the assumption (1), the changes of the transverse strain ε_t , and the shear strain ε_{lt} are ignored. The longitudinal strain ε_l expression specified underneath by Equation (3) is achieved after the transformation relation shown by Equation (2).

$$\varepsilon_l = c^2 \varepsilon_x + s^2 \varepsilon_\theta + sc \varepsilon_{x\theta} \tag{3}$$

The appropriate angle is replaced in Equation (3) to achieve the strains throughout all the stiffener orientation. Whereas in the circumstance of an iso-grid stiffener procedure such angles relate to 0° , 60° , & -60° . When the axial strains happening the stiffeners are originated, the consistent axial forces specifically F_1 , F_2 , F_3 remain computed since the longitudinal strains, cross-sectional area and longitudinal modulus (E_l) of the stiffeners. Bring up to Fig.2 aimed at the force-free body figure of the unit cell. Equation (4) appended expressions the resulting three forces.

$$\begin{aligned} F_1 &= AE_l \varepsilon_{l1} = AE_l (c^2 \varepsilon_x + s^2 \varepsilon_\theta + sc \varepsilon_{x\theta}) \\ F_2 &= AE_l \varepsilon_{l2} = AE_l (c^2 \varepsilon_x + s^2 \varepsilon_\theta + sc \varepsilon_{x\theta}) \\ F_3 &= AE_l \varepsilon_{l3} = AE_l (\varepsilon_\theta) \end{aligned} \tag{4}$$

The resultant forces on every edge of the unit cell are computed through the vectorial addition of the forces of the stiffeners. Summing up the x-direction forces on whichever the top or bottom side of the unit cell effects in Equation (5).

$$F_x = F_1 \cos(\alpha) + F_2 \cos(\alpha) \tag{5}$$

Likewise summing up hoop path forces on either the left or right side of the unit cell effect in Equation (6).

$$F_\theta = F_1 \sin(\alpha) + F_2 \sin(\alpha) + 2F_3 \tag{6}$$

The expression of the shear force ($F_{x\theta}$), is done by addition of the force constituents throughout whichever of the rims of the unit cell. Execution of this on one of the vertical sides yields Equation (7).

$$F_{x\theta} = F_2 \cos(\alpha) - F_1 \cos(\alpha) \tag{7}$$

The similar shear force equation will outcome level if the horizontal face is employed in its place of the vertical face meanwhile of the geometrical relationships among ‘a’, ‘b’, $\cos(\alpha)$, and $\sin(\alpha)$.

Replacing Equation (4) by Equations (5), (6), (7):

$$\begin{aligned} F_x &= AE_l c (c^2 \varepsilon_x + s^2 \varepsilon_\theta + sc \varepsilon_{x\theta}) + AE_l c (c^2 \varepsilon_x + s^2 \varepsilon_\theta + sc \varepsilon_{x\theta}) \\ &= AE_l (2c^2 \varepsilon_x + 2s^2 \varepsilon_\theta + 2sc \varepsilon_{x\theta}) \\ F_\theta &= AE_l s (c^2 \varepsilon_x + s^2 \varepsilon_\theta + sc \varepsilon_{x\theta}) + AE_l s (c^2 \varepsilon_x + s^2 \varepsilon_\theta + sc \varepsilon_{x\theta}) + AE_l (\varepsilon_\theta) \\ &= AE_l s (sc^2 \varepsilon_x + s^3 \varepsilon_\theta + 2sc \varepsilon_{x\theta}) \\ F_{x\theta} &= AE_l c (c^2 \varepsilon_x + s^2 \varepsilon_\theta + sc \varepsilon_{x\theta}) - AE_l c (c^2 \varepsilon_x + s^2 \varepsilon_\theta + sc \varepsilon_{x\theta}) \\ &= AE_l (-sc^2 \varepsilon_x) \end{aligned} \tag{8}$$

Here resultant forces, i.e. the force per unit length N_x , N_θ , and $N_{\theta x}$, are reached through dividing the overhead force equations through the resultant edge width of the unit cell. Later executions of this and replacing the strain relations as of Equation (1), equations used for the resultant forces preceding the unit cell remain reached.

$$N_x = \frac{AE_l}{a} \left[2c^3 \varepsilon_x^0 + 2c^3 k_x \left(\frac{t}{2}\right) + 2s^2 c \varepsilon_\theta^0 + 2c^2 c k_\theta \left(\frac{t}{2}\right) \right]$$

$$N_{\theta} = \frac{AEt}{b} \left[2sc^2 \epsilon_x^o + 2sc^3 k_x \left(\frac{t}{2} \right) + (2s^2 + 2) \epsilon_{\theta}^o + (2s^2 + 2) k_{\theta} \left(\frac{t}{2} \right) \right] \quad (9)$$

$$N_{\theta x} = \frac{AEt}{b} \left[2sc^2 \epsilon_{x\theta}^o + 2sc^3 k_{x\theta} \left(\frac{t}{2} \right) \right]$$

B. Moment Analysis[6]

The moments because to the stiffeners are originated through the shear forces on the crossing point of the shell and the stiffeners. Since stability, these shear forces equivalent to the forces on the stiffeners computed in the earlier segment. The moment exaggerated by such forces on the midplane of the shell the same the forces multiplied through one-half the shell thicknesses. Moment free body schematic in Fig.3 shows the dissimilar moments created through this force F. First M_{sh} is of foremost attention Mean while it is the moment consequence of the shear forces on the shell. It can be detected later the free body diagram a net moment M effects on the shell/stiffener assembly. This moment indicates the coupling of moment and force resulting from the non-symmetric structure of the shell/stiffener preparation.

Fig.4 illustrations moment free body diagram of a unit cell. M_1 , M_2 , and M_3 remain the moments causing from forces F_1 , F_2 , and F_3 correspondingly.

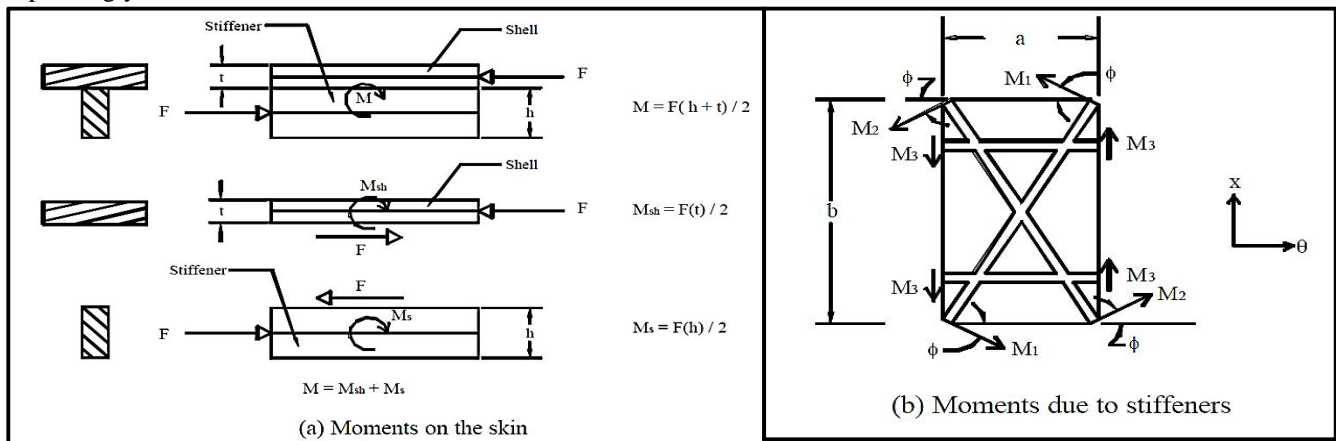


Fig.3 Skin Moments Diagram

Fig.4 Rib Moments Diagram

Subsequent the similar procedure as the force analysis on a unit cell, the resultant moments on the horizontal and vertical sides of the unit cell are computed.

$$M_x = M_1 \cos(\phi) + M_2 \cos(\phi) \quad (10a)$$

$$M_{y\phi} = M_1 \sin(\phi) + M_2 \sin(\phi) + 2M_3 \quad (10b)$$

$$M_{x\phi} = M_2 \cos(\phi) - M_1 \sin(\phi) \quad (10c)$$

The moments M_1 , M_2 , and M_3 are computed through multiplying the consistent shear forces (F_1 , F_2 , and F_3) through the lever arm, which is half the thickness of the shell. Creating such substitutes meant for the moments and dividing through the consistent edge lengths drive result in the resultant moments. Expression (11) illustrates the final effect later interpretation.

$$M_x = \frac{AEt}{2a} \left[2c^3 \epsilon_x^o + 2c^3 k_x \left(\frac{t}{2} \right) + 2s^2 c \epsilon_{\theta}^o + 2c^2 c k_{\theta} \left(\frac{t}{2} \right) \right]$$

$$M_{\theta} = \frac{AEt}{2b} \left[2sc^2 \epsilon_x^o + 2sc^2 k_x \left(\frac{t}{2} \right) + (2s^3 + 2) \epsilon_{\theta}^o + (2s^3 + 2) k_{\theta} \left(\frac{t}{2} \right) \right] \quad (11)$$

$$M_{\theta x} = \frac{AEt}{2b} \left[2sc^2 \epsilon_{x\theta}^o + 2sc^2 k_{x\theta} \left(\frac{t}{2} \right) \right]$$

C. The Stiffness Matrix[6]

Here both the equations (9) and (11) stand correspondingly the force and moment offerings of the stiffener, hereafter forth specified through the superscripts. These expressions stand précised in a matrix arrangement in Expression (12). The resultant matrix elements remain purposes of the midplane strains and curvatures of the shell. These remained resultant through investigating the force and moments in line for stiffeners. We specify such stiffness parameters as $A_{ij}^s, B_{ij}^s, C_{ij}^s$.

$$\begin{bmatrix} N_x^s \\ N_\theta^s \\ N_{x\theta}^s \\ M_x^s \\ M_\theta^s \\ M_{x\theta}^s \end{bmatrix} = AE_l \begin{bmatrix} \frac{2c^3}{a} & \frac{2s^3c}{a} & 0 & \frac{c^3t}{a} & \frac{s^2ct}{a} & 0 \\ \frac{2sc^2}{b} & \frac{2(sc^3+2)}{b} & 0 & \frac{sc^2t}{b} & \frac{(2s^3+2)t}{2b} & 0 \\ 0 & 0 & \frac{2sc^2}{b} & 0 & 0 & \frac{sc^2t}{b} \\ \frac{c^3t}{a} & \frac{s^2ct}{a} & 0 & \frac{c^3t}{2a} & \frac{s^2ct2}{2a} & 0 \\ \frac{sc^2t}{b} & \frac{(2s^3+2)t}{2b} & 0 & \frac{sc^2t^2}{2b} & \frac{(2s^2+2)t^2}{4b} & 0 \\ 0 & 0 & \frac{sc^2t}{b} & 0 & 0 & \frac{sc^2t^2}{2b} \end{bmatrix} \begin{bmatrix} \epsilon_x^o \\ \epsilon_\theta^o \\ \epsilon_{x\theta}^o \\ k_x \\ k_\theta \\ k_{x\theta} \end{bmatrix} \quad (12)$$

By principal glimpse the stiffness matrix specified through Expression (12) influencing seem unsymmetrical (i.e. $A_{ij} \neq A_{ji}$ and $D_{ij} \neq D_{ji}$), on the other hand because of the geometric relative among the parameters 'a', 'b', $\cos(\phi)$ and $\sin(\phi)$ these stiffness quantities are been revealed to be equal. It can moreover remain detected the identical B_{ij} elements end since the autonomous force and moment analysis on the unit cell. It is in decent procedure with laminate theory, hereafter further authorizing the early expectations ended.

Total force and moment of the panel remain the superposition of the force and moment because of the stiffener also the shell. These extents can stay straight covered, as the stiffener force and moment offerings must remain advanced relay on the midplane strains and curvatures. The rule of combinations is applied and the moments and forces remain covered allowing toward the volume fractions of the stiffeners and the shell of Expression 13. V_s and V_{sh} view for the volume fraction of stiffener and shell correspondingly.

$$\begin{bmatrix} N \\ M \end{bmatrix} = \begin{bmatrix} V_s N^s & + V_{sh} N^{sh} \\ V_s M^s & + V_{sh} M^{sh} \end{bmatrix} \quad (13)$$

In matrix expression 13 N_{sh} and M_{sh} are the force and moment influence of the shell correspondingly. These extents are simply computed through smearing the laminate theory on the shell. Replacing force and moment terminologies for the stiffener network from Equation (12) and the resultant terminologies for the shell after the laminate theory results in the panel constitutive expression specified through Expressions 14. In this expression A, B and D signify the extensional, coupling, and bending stiffness quantities correspondingly.

$$\begin{bmatrix} N \\ M \end{bmatrix} = \begin{bmatrix} V_s A^s + V_{sh} A^{sh} & | & V_s B^s + V_{sh} B^{sh} \\ V_s B^s + V_{sh} B^{sh} & | & V_s D^s + V_{sh} D^{sh} \end{bmatrix} \begin{bmatrix} \epsilon^o \\ k \end{bmatrix} \quad (14)$$

Resultant stiffness parameters achieved from Expression 14 endure therefore the equivalent stiffness parameters of the total panel.

D. Buckling Load Calculation[6]

Ritz method is implemented to compute the buckling load of the cylinder [14]. The entire potential energy of the cylinder π remains the totaling of the strain energy U and the effort finished through the external force V.

The strain energy on behalf of an orthotropic cylinder is certain through Expression (15) underneath [14].

$$\begin{aligned} U = & \frac{1}{2} \int_0^{2\pi r} \int_0^L \left\{ A_{11} \left(\frac{\partial u}{\partial x} \right)^2 + 2A_{12} \frac{\partial u}{\partial x} \left(\frac{\partial u}{\partial x} + \frac{w}{r} \right) + A_{22} \left[\frac{\partial v}{\partial \theta} \left(\frac{\partial v}{\partial \theta} + \frac{w}{r} \right) + \left(\frac{w}{r} \right)^2 \right] \right. \\ & + 2 \left[A_{16} \frac{\partial v}{\partial \theta} + A_{26} \left(\frac{\partial v}{\partial \theta} + \frac{w}{r} \right) \right] \left(\frac{\partial v}{\partial \theta} + \frac{\partial u}{\partial x} \right) + A_{66} \left(\frac{\partial u}{\partial \theta} + \frac{\partial v}{\partial x} \right)^2 - B_{11} \frac{\partial u}{\partial x} + \frac{\partial^2 w}{\partial x^2} \\ & - 2B_{12} \left[\left(\frac{\partial v}{\partial \theta} + \frac{w}{r} \right) \frac{\partial^2 w}{\partial x^2} + \frac{\partial u}{\partial x} + \frac{\partial^2 w}{\partial x^2} \right] - B_{22} \left(\frac{\partial v}{\partial \theta} + \frac{w}{r} \right) \frac{\partial^2 w}{\partial \theta^2} - 2B_{16} \left[\frac{\partial^2 w}{\partial x^2} \left(\frac{\partial u}{\partial \theta} + \frac{\partial v}{\partial x} \right) + 2 \frac{\partial u}{\partial x} \frac{\partial^2 w}{\partial x \partial \theta} \right] \\ & - 2B_{26} \left[\frac{\partial^2 w}{\partial \theta^2} \left(\frac{\partial u}{\partial \theta} + \frac{\partial v}{\partial x} \right) + 2 \left(\frac{\partial v}{\partial \theta} + \frac{w}{r} \right) \frac{\partial^2 w}{\partial x \partial \theta} \right] - 4B_{66} \frac{\partial^2 w}{\partial x \partial \theta} \left(\frac{\partial u}{\partial x} + \frac{\partial v}{\partial \theta} \right) + D_{11} \left(\frac{\partial^2 w}{\partial x^2} \right)^2 \\ & \left. + 2D_{12} \frac{\partial^2 w}{\partial x^2} \frac{\partial^2 w}{\partial \theta^2} + D_{22} \left(\frac{\partial^2 w}{\partial \theta^2} \right)^2 + 4 \left(D_{16} \frac{\partial^2 w}{\partial x^2} + D_{26} \frac{\partial^2 w}{\partial \theta^2} \right) \frac{\partial^2 w}{\partial x \partial \theta} + 4D_{66} \left(\frac{\partial^2 w}{\partial x \partial \theta} \right)^2 \right\} dx d\theta \quad (15) \end{aligned}$$

This strain energy is there a purpose of the equivalent stiffness parameters of the cylinder panel, the radius of the cylinder 'r' and the unidentified movement fields in the radial, axial and hoop direction 'w', 'u' and 'v' correspondingly. Meanwhile, the stiffened cylinder panel has remained reduced to an equivalent orthotropic laminate; Expression (15) is been adapted straight. The potential energy because of in-plane load remains in chance specified by Expression (16) below. In Expression (16) N remains the load per unit length smeared on the rim of the cylinder.

$$v = \frac{1}{2} \int_0^{2\pi r} \int_0^L N_\theta \left(\frac{\partial w}{\partial x}\right)^2 dx d\theta \tag{16}$$

The total energy of the cylinder is obtained by the strain energy ‘U’ and the potential energy term ‘V’ stand combined beside the circumference and the height ‘H’ of the cylinder.

The displacement field u, v and w, are stand definite through kinematically acceptable functions, i.e., displacement fields satisfying the necessary boundary conditions. Hereafter they are projected through a double Fourier series that gratify the boundary condition necessities. On behalf of a simply supported end condition the displacement fields are specified through Expression (17) below [16],

$$\begin{aligned}
 u &= \sum_{m=1}^{\infty} \sum_{n=1}^{\infty} A_{mn} \cos(\bar{m}x) \sin(\bar{n}s) \\
 v &= \sum_{m=1}^{\infty} \sum_{n=1}^{\infty} B_{mn} \sin(\bar{m}x) \cos(\bar{n}s) \\
 w &= \sum_{m=1}^{\infty} \sum_{n=1}^{\infty} C_{mn} \sin(\bar{m}x) \sin(\bar{n}s)
 \end{aligned} \tag{17}$$

$$\bar{m} = m\pi/L, \bar{n} = n/r, s = r\theta, L = \text{height of cylinder and } m, n = 1, 2, 3, \dots$$

Although on behalf of a clamped boundary condition the expression for u, v and w are specified through Eqn. (18)

$$\begin{aligned}
 u &= \sum_{m=1}^{\infty} \sum_{n=1}^{\infty} A_{mn} \cos(\bar{m}x) \sin(\bar{n}s) \\
 v &= \sum_{m=1}^{\infty} \sum_{n=1}^{\infty} B_{mn} \sin(\bar{m}x) \cos(\bar{n}s) \\
 w &= \sum_{m=1}^{\infty} \sum_{n=1}^{\infty} C_{mn} (1 - \cos(\bar{m}x)) \sin(\bar{n}s)
 \end{aligned} \tag{18}$$

$$\bar{m} = m\pi/L, \bar{n} = n/r, s = r\theta, \text{ and } m, n = 1, 2, 3, \dots$$

When the displacement fields remain definite, they are replaced by Expression (15) and (16) Combined between the limits of integration. We add the following expressions of the strain energy and the work done through the in-plane load and discover an overall expression on behalf of the total energy of the system. The total energy expression is a purpose of the stiffness matrix elements of the equivalent laminate and the unidentified displacement field constants A_{mn} , B_{mn} and C_{mn} . Used for the equilibrium to stand stable, the total potential energy of the system essential are smallest. It can be satisfied by means of the outcome of the first derivative of the total potential energy by reference to the unidentified coefficients A_{mn} , B_{mn} and C_{mn} and equate to zero. It fallouts in an eigen value problem.

E. Vibrational analysis and Structural response[11]

Considering the cylindrical shell with constant thickness t, radius R, and length L. Middle surface of the skin is taken as a reference surface of the where an orthogonal coordinate system (x, θ, z) is fixed. As shown in Fig.5, the x-axis is taken in the axial direction of the shell, where the θ and z-axes are in the circumferential and radial directions of the shell, respectively. The displacements of the shell are taken as u, v, w in the x, θ, z directions respectively. The equations of motion for a cylindrical shell can be written by the Love theory in the matrix expression 19:

$$\begin{bmatrix} L_{11} & L_{12} & L_{13} \\ L_{21} & L_{22} & L_{23} \\ L_{31} & L_{32} & L_{33} \end{bmatrix} \begin{Bmatrix} u \\ v \\ w \end{Bmatrix} = \begin{Bmatrix} 0 \\ 0 \\ 0 \end{Bmatrix} \tag{19}$$

Where: $L_{ij}(i, j = 1, 2, 3)$ – the differential operators with respect to x and θ.

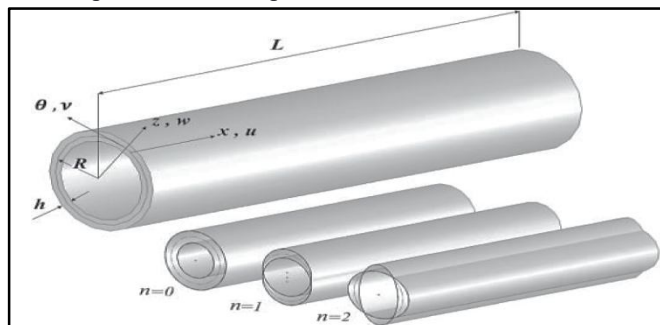


Fig.5 Co-ordinate system and circumferential modal shape [17]

Due to the satisfaction of the boundary conditions, the displacement u, v and w can be explained as double Fourier series [11]

$$\begin{aligned}
 u(x, \theta, t) &= \sum_m \sum_n A_{mn} \frac{\partial \phi_u(x)}{\partial x} \cos(n\theta) \cos(\omega t) \\
 v(x, \theta, t) &= \sum_m \sum_n B_{mnv} \phi(x) \sin(n\theta) \cos(\omega t) \\
 u(x, \theta, t) &= \sum_m \sum_n C_{mnw} \phi(x) \cos(n\theta) \cos(\omega t) \tag{20}
 \end{aligned}$$

In recent equations, A_{mn} , B_{mn} and C_{mn} are coefficients of natural modes shape, which obtained from solving free vibration. For solving free vibrations, $T_{mn}(t) = e^{\omega_{mn}t}$ is considered as a function of time, m is the number of axial half-wavelength, n is the number of circumferential half-wavelength and ω_{mn} is the natural frequency in the mode of mn . To satisfy boundary conditions, axial and circumferential functions are explained as below.

$$\begin{cases}
 \phi_i(x) = \alpha_1 \cosh\left(\frac{\lambda_m x}{L}\right) + \alpha_2 \cos\left(\frac{\lambda_m x}{L}\right) - \sigma_m \left(\alpha_3 \sinh\left(\frac{\lambda_m x}{L}\right) - \alpha_4 \sin\left(\frac{\lambda_m x}{L}\right) \right) \\
 \phi_v(\theta) = \sin(n\theta) \quad \phi_u(\theta) = \phi_w(\theta) = \cos(n\theta)
 \end{cases} \quad (i = u, v, w)$$

In above equations, α_i are constant coefficients which determined according to boundary conditions. λ_m is the root of non-linear equations and σ_m is the dependent parameter on λ_m which obtained according to boundary conditions. Free-Free supported conditions can be defined as below.

$$\frac{\partial^2 \phi(x)}{\partial x^2} = \frac{\partial^3 \phi(x)}{\partial x^3} = 0$$

1) *Free Vibration Analysis*[11]: Using Galerkin method and substituting Equation 20 into Equation 19, it can be written as:

$$\begin{bmatrix} c_{11} & c_{12} & c_{13} \\ c_{21} & c_{22} & c_{23} \\ c_{31} & c_{32} & c_{33} \end{bmatrix} \begin{Bmatrix} A_{mn} \\ B_{mn} \\ D_{mn} \end{Bmatrix} = 0 \tag{21}$$

Where $C_{ij}(i, j = 1, 2, 3)$ – the parameters from the L_{ij} after they are operated with the x and θ .

For non-trivial solutions, one sets the determinant of the characteristic matrix in Equation 21 to zero:

$$|C_{ij}| = 0 \quad (i, j = 1, 2, 3) \tag{22}$$

So the frequency equation can be obtained as:

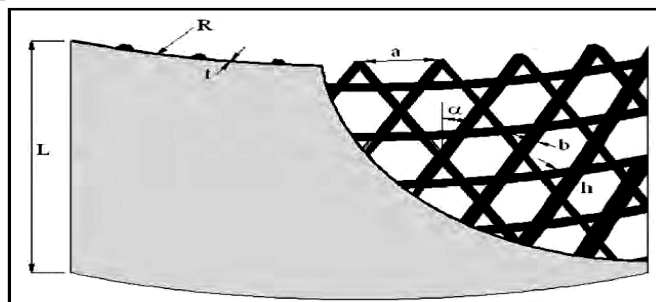
$$\beta_1 \omega^6 + \beta_2 \omega^4 + \beta_3 \omega^2 + \beta_4 = 0 \tag{23}$$

where $\beta_i(i, j = 1, 2, 3)$ – the coefficients of Equation. 22.

Solving Equation 23, one obtains three positive roots and three negative roots. The three positive roots are the angular natural frequencies of the cylindrical shell in the axial, circumferential and radial directions. The lowest of the three positive roots represents the flexural vibration, and the other two are in-plane vibrations.

III. PARAMETRIC DESIGN

Various parameters in Fig.6 associated with a cylindrical grid-stiffened structure can be listed as length L , radius R , kind of grid arrangement, height of stiffening ribs h , width of stiffening rib b , orientation of helical ribs a , number of stiffening ribs, distance among stiffening ribs a besides thickness t and ply arrangement of skin, etc[1]. Particular the length and radius of the structure, an optimal design implementation is fundamentally that of influential the design parameters that withstand the design loads with the desired factor of safety and least mass. For a cylinder of radius R subjected to axial compression F and bending moment M , the design load P is in use [18]:



$$P = F + \frac{2M}{R} \tag{24}$$

Fig.6 Design parameters panel of a grid-stiffened cylinder



10.22214/IJRASET



45.98



IMPACT FACTOR:
7.129



IMPACT FACTOR:
7.429



INTERNATIONAL JOURNAL FOR RESEARCH

IN APPLIED SCIENCE & ENGINEERING TECHNOLOGY

Call : 08813907089  (24*7 Support on Whatsapp)